JOURNAL OF SYNCHROTRON RADIATION
ISSN 1600-5775

Application of interference fits on cylindrical monochromator crystals to overcome clamping and cooling deformations

Joshua Stimson,[a]* Michael Ward,[a] John Sutter,[b] Sofia Diaz-Moreno,[b] Simon Alcock[b] and Peter Docker[b]

[a]School of Engineering and the Built Environment, Birmingham City University, Curzon Street, Birmingham, West Midlands B4 7XG, UK, and [b]Diamond Light Source, Fermi Avenue, Didcot OX11 0DE, UK. *Correspondence e-mail: joshua.stimson@bcu.ac.uk

Received 11 October 2018
Accepted 21 January 2019

Edited by S. Svensson, Uppsala University, Sweden

Keywords: monochromator design; interference fit; first crystal cooling.

In order to provide adequate cryogenic cooling of both existing and next-generation crystal monochromators, a new approach to produce an optimum thermal interface between the first crystal and its copper heat exchanger is proposed. This will ensure that the increased heat load deposited by higher X-ray powers can be properly dissipated. Utilizing a cylindrical silicon crystal, a tubular copper heat exchanger and by exploiting the differing thermal and mechanical properties of the two, a very good thermal interface was achieved at liquid-nitrogen temperatures. The surface flatness of the diffracting plane at one end of the cylindrical crystal was measured at room temperature while unconstrained. The crystal was then placed into the copper heat exchanger, a slide fit at room temperature, and then cooled to liquid-nitrogen temperature. At −200°C the slide fit became an interference fit. This room-temperature 'loose' fit was modelled using finite-element analysis to obtain the desired fit at cryogenic temperatures by prescribing the fit at room temperature. Under these conditions, the diffraction surface was measured for distortion due to thermal and mechanical clamping forces. The total deformation was measured to be 30 nm, an order of magnitude improvement over deformation caused by cooling alone with the original side-clamped design this concept method is set to replace. This new methodology also has the advantage that it is repeatable and does not require macro-scale tools to acquire a nanometre-accuracy mounting.

1. Introduction

As synchrotrons see more varied use (Wilson, 1996), it is beneficial to optimize the usage of space by spurring additional beamlines off existing ones. A major limit to this, however, is the size of the optics; in order to minimize the effect of deformations introduced through clamping and cooling monochromator assemblies it is industry practice to make monochromator crystals significantly larger than the footprint of the beam incidental on the surface, often by a factor of two or more (Bilderback *et al.*, 2000).

In addition, there is a demand for greater powers to be generated at the synchrotrons as the incident power has a directly proportional relation to the resolution of any generated image and the minimum sample size of any detected material (Odier *et al.*, 2009). The traditional response to the use of higher powers has been to increase the size of the crystal such that the diffracting surface in the beam footprint fits within the relatively flat central section.

The vast majority of monochromator assemblies are composed of a silicon crystal held within copper heat exchangers by use of steel or invar bolts, often with a foil of indium between the copper and silicon to mitigate some of the

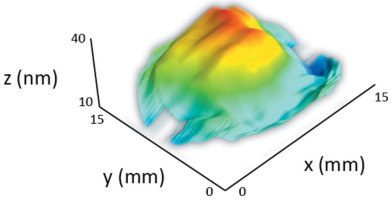

deformation and improve thermal contact (Bilderback *et al.*, 2000; Carpentier *et al.*, 2001). By introducing three sets of independent material properties, such as thermal expansion coefficients and heat capacities, this introduces not only clamping pressures and torque when the components are assembled but also causes the elements of the assembly to deform thermally at different rates.

In this work, we suggest a novel solution to the aforementioned issues: the use of a cylindrical silicon crystal, held in a cylindrical copper sleeve manufactured such that the two bodies are in loose mechanical contact at room temperature, yet in good intimate contact at cryogenic temperatures. This will give a lower uniform stress distribution and avoid complex mechanical clamping procedures and stresses.

2. Theory

The theory behind the novel design has been examined in detail in a previous paper by Stimson *et al.* (2017), and so only a brief review will be detailed here.

The core concept behind an interference fit is well known (Tipler, 1999); by causing two objects to attempt to occupy the same space, usually by either forcing the two bodies together mechanically or enlarging one object thermally such that it contracts into the other's space when cooled, we can induce a very high, uniform stress field. However, due to the drastically different thermal expansion coefficients of silicon and copper (Petersen, 1982; Shah & Straumanis, 1972; NIST, 1992; Middelmann *et al.*, 2015) and the very low temperatures used in synchrotron monochromators (Carpentier *et al.*, 2001), we find that to cause an interference fit at room temperature causes destructively high pressures when cooled. Instead, by cooling the copper to liquid-nitrogen temperatures (approximately 80 K) we can cause the copper sleeve to contract faster and to a greater degree than the silicon, forming a uniform, high-pressure mechanical and thermal contact across the entirety of the inner surface of the copper sleeve. Previous work (Stimson *et al.*, 2017) found that the appropriate room-temperature gap was approximately 30 µm between the silicon and copper at all points, producing a uniform stress field of the order of 10^8 Pa. This was required to provide optimal thermal contact with minimal mechanical deformation.

3. Method

In order to test the new design, a number of cylindrical crystals and heat-exchanger sleeves were manufactured. The crystals had a radius of 12.5 mm and a length of 50 mm; they were marginally tapered, presenting a slightly conical profile; as such, the narrow ends were polished such that any latitudinal movement was directed away from the polished surface. The sleeves matched the slope of the crystal, with an internal radius of 12.53 mm, an external radius of 17.53 mm and a length of 40 mm, and brass stoppers with a length of 8 mm and a radius of 3 mm for the first 5 mm of length and a radius of 6 mm for the remaining 3 mm of length secured on stainless steel AISI 304 bolts were fitted to the bottom of the sleeves to ensure the appropriate fit was achieved. The crystal was inserted such that the optically polished flat end of the cylinder extended approximately 5 mm beyond the level of the copper heat exchange, forming the crystal assembly shown in Fig. 1.

This assembly was inserted into a vacuum vessel, held in location by a copper clamp attached to a hollow copper tube referred to as the 'cold finger'. The cold finger extends through the vacuum vessel and terminates within a stainless steel receptacle; by filling the receptacle with liquid nitrogen, we could rapidly cool the assembly to −190°C. An optical grade window on the front of the vacuum vessel allowed a direct view of the diffracting surface of the crystal shown in Fig. 2. The vessel was aligned in front of a mini-Fizeau interferometer, which was used to measure the flatness of the diffracting surface.

The crystal–sleeve assembly was imaged at room temperature without vacuum, at room temperature at 10^{-8} mbar and at liquid-nitrogen temperatures (approximately −190°C) under vacuum. The surface profile imaged at room temperature under vacuum was subtracted from that imaged at liquid-nitrogen temperatures under vacuum to find the deformation caused by the system cooling and the copper clamping the silicon.

The sleeve illustrated in Fig. 1 featured a 30 µm room-temperature gap between the crystal and sleeve. The assembly was tested multiple times to ensure results were repeatable.

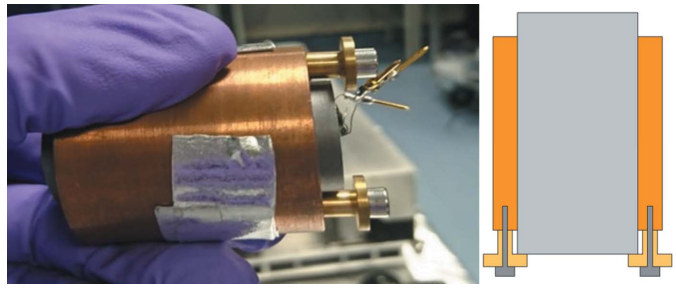

Figure 1
Left: cylindrical single-crystal (111) silicon in a copper heat-exchanger sleeve. Right: cross-sectional diagram of a silicon crystal in a copper heat exchanger sleeve. Steel bolts fix the brass stoppers in place to hold the crystal in the heat exchanger.

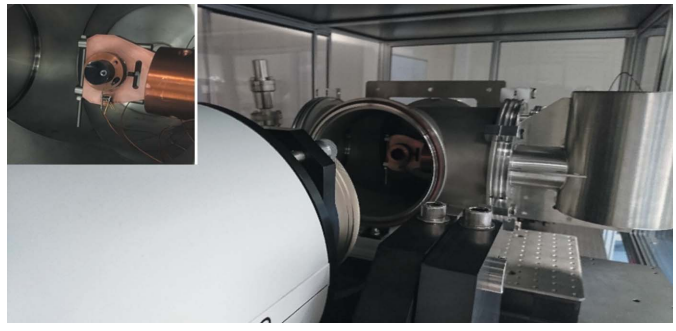

Figure 2
Crystal assembly contained in a vacuum vessel placed in view of a mini-Fizeau interferometer. The liquid-nitrogen receptacle for the cold finger is visible on the right. Insert: close-up of the crystal assembly.

4. Results

The crystal was measured at room temperature and atmospheric pressure; it was found to have a saddle-shaped deformation with a maximum height difference of 850 nm, as shown in Fig. 3.

The vessel was pumped down to 10^{-8} mbar and the crystal surface was imaged again; there was no significant difference in the crystal surface measurement between atmospheric pressure and under vacuum. Liquid nitrogen was then introduced to the cold finger, and the temperature of the crystal and sleeve was measured using PT100 temperature sensors until they reached equilibrium with the cold finger, around −190°C after an hour of cooling.

The temperatures of both the crystal and sleeve were measured as the system cooled, as shown in Fig. 4 below. Fig. 4 also shows the gap between the copper and the silicon, calculated using the thermal expansion coefficient of each material integrated over the change in temperature, to compare the internal radius of the copper sleeve with the radius of the silicon crystal; once this line drops below zero, the two bodies are forced into an interference fit regime. There is a visible turning point in the temperature of the silicon crystal at 500 s; this is the point at which the copper shrank sufficiently to form good thermal contact with the silicon, approximately 10 µm. The silicon continues to cool faster than the copper until the two are in ideal thermal contact at 800 s, which correlates to a shrinkage of 60 µm, *i.e.* the two bodies coming into interference.

Once cooled, the crystal surface was measured again. The room-temperature scan was subtracted from the cryogenic-temperature scan to find the deformation induced in the surface of the crystal due to cooling and clamping. It is worth noting that we cannot separate cooling and clamping deformations by design, as cooling the sleeve is what causes it to clamp the crystal.

Fig. 5 shows that the total deformation across the entire crystal surface is approximately 30 nm.

In contrast, the conventional side-clamped first monochromator crystal assembly used at the I20 beamline at Diamond Light Source was measured in the same manner (Docker *et al.*, 2013), and deformation from cooling was found in some cases to be as high as 400 nm, an order of magnitude higher (see Fig. 6). It should be noted that these earlier measurements were taken between a clamped room-temperature assembly and a clamped cryogenic assembly, and so would not show the deforming effect of clamping. These earlier tests also relied on interfaces containing indium. It is important to note that these tests also highlighted the fact that

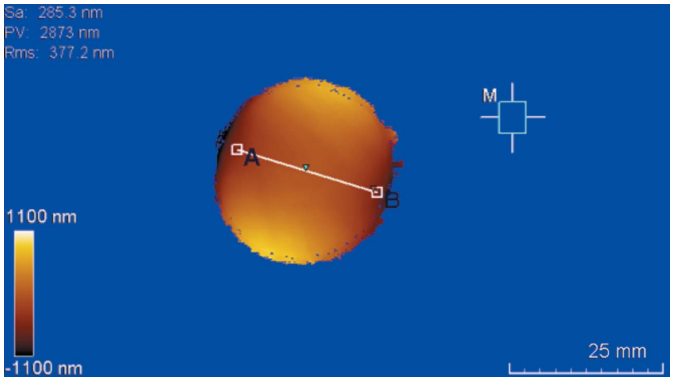

Figure 3
Room-temperature atmospheric-pressure surface profile of the silicon crystal, showing a maximum difference of 850 nm.

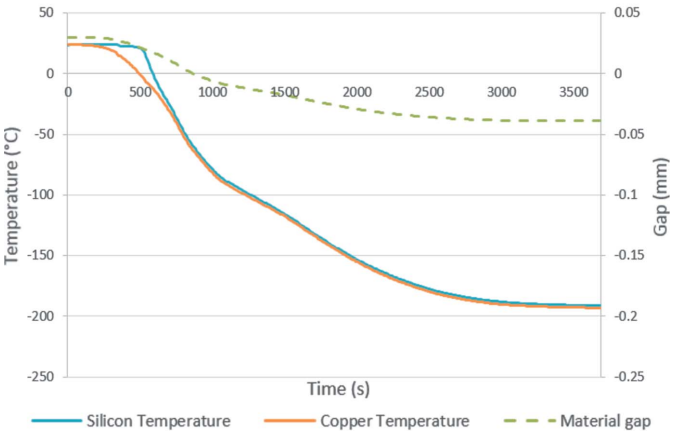

Figure 4
Left axis: temperature of silicon crystal and copper heat exchange as a function of time. Right axis: calculated gap between copper and silicon as a function of time; a negative gap indicates the two materials are interfering.

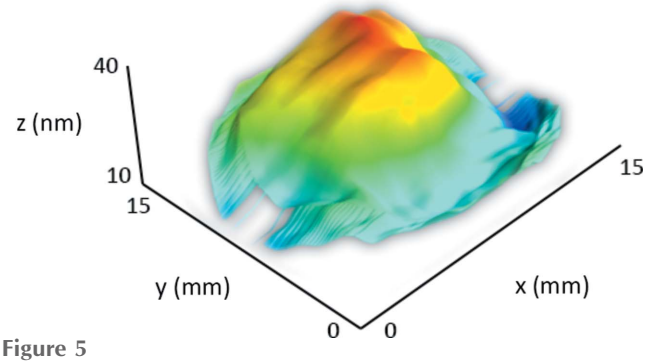

Figure 5
Surface deformation caused in the crystal by cooling and clamping. Image created by subtracting the crystal image at 27°C from the crystal image at −190°C, showing a 30 nm deformation across the diffracting area.

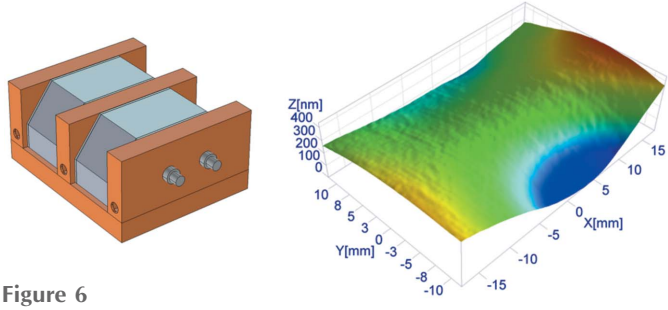

Figure 6
Left: conventional side-clamped first monochromator crystal assembly used at the I20 beamline at Diamond Light Source. Right: surface deformation caused in the crystal by cooling of the standard assembly. Image created by subtracting the crystal image at 27°C from the crystal image at −190°C, showing a 400 nm deformation across the diffracting area.

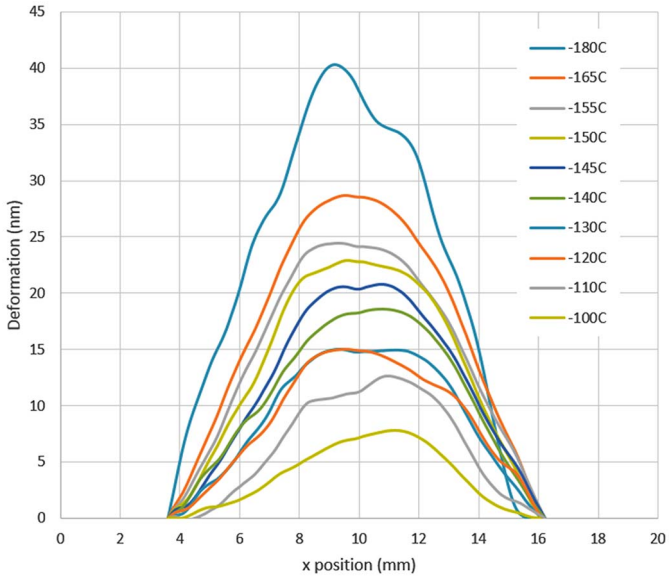

Figure 7
Deformation observed in the silicon diffracting surface as the crystal was heated to room temperature. Significant deformation is observed between −155°C and −180°C.

conventional assembly is not repeatable; multiple repetitions of the same assembly yielded remarkably different results, highlighting the unreliability of such an approach.

The assembly was then allowed to return to room temperature and the procedure was repeated showing a negligible difference between the results for each repetition. The crystal was also removed from the assembly, inspected for deformations or damage and returned, and the procedure was repeated once more resulting in another negligible difference. Finally, the surface profile of the crystal was recorded as the assembly was heated from −200°C to room temperature. Fig. 7 shows the surface profile of the crystal during heating after cooling.

There is a visible dramatic increase in deformation below −155°C; the maximum deformation grows from 0 nm at 27°C to 25 nm at −155°C, a difference of 25 nm over a range of 182°C, while it grows to over 40 nm by −180°C, a difference of 15 nm over just 25°C. This is of interest as −155°C correlates to 120 K, a temperature at which silicon shows a coefficient of thermal expansion of zero. This is the 'ideal' temperature to run a first crystal in service. The cause of this sudden deformation is the thermal expansion coefficient of silicon, which dips below 0 at −150°C. This suggests that at temperatures this low the silicon effectively grows as the temperature falls, creating further stress within the interference fit. This additional stress can be modelled using finite-element analysis software, though this has been left for future work at this stage.

5. Discussion

The low surface deformation caused by the new proposed clamping methodology presented in this paper demonstrates great promise. When compared with the side-clamping regime it is proposing to replace, the interference fit design can offer an order of magnitude improvement in terms of the deformation of the diffracting surface for Bragg diffraction. In addition, the repetition demonstrated shows that the crystal can be a 'set and forget' system, assembled once and losing no quality or efficiency over repeated cooling cycles. The design presented herein can also be assembled once and then maintained as such indefinitely as the tapered crystal and brass stops prevent the crystal dislocating from the heat exchanger.

A very strong thermal contact was achieved, as shown by the temperature of the heat exchanger and the crystal rapidly reaching equilibrium over no longer than 15 min, and maintaining a temperature difference of less than 4°C after the interference fit; this indicates a strong thermal contact, theoretically suitable for even higher heat loads than are currently utilized in synchrotron devices.

Considered together, these results indicate that the novel design suggested here, of a cylindrical silicon crystal located within a sleeve-shaped copper heat exchanger such that an interference fit is created upon cooling to liquid-nitrogen temperatures, is a revolutionary design when compared with the conventional monochromator assembly. Further work will focus on the introduction of X-ray beams and heaters to test the performance of the monochromator as a Bragg diffractor under various thermal loads, as well as modelling the stresses present within the crystal.

Funding information

The following funding is acknowledged: Diamond Light Source; Birmingham City University.

References

Bilderback, D. H., Freund, A. K., Knapp, G. S. & Mills, D. M. (2000). *J. Synchrotron Rad.* **7**, 53–60.
Carpentier, P., Rossat, M., Charrault, P., Joly, J., Pirocchi, M., Ferrer, J. L., Kaïkati, O. & Roth, M. (2001). *Nucl. Instrum. Methods Phys. Res. A*, **456**, 163–176.
Docker, P., Alcock, S. & Nistea, I. (2013). Unpublished.
Middelmann, T., Walkov, A., Bartl, G. & Schödel, R. (2015). *Phys. Rev. B*, **92**, 174113.
NIST (1992). *National Institute of Standards and Technology Monograph 270*. NIST, Gaithersburg, MD, USA.
Odier, P., Thoulet, S. & Ludwig, M. (2009). *Proceedings of Beam Diagnostics and Instrumentation for Particle Accelerators*, 25–27 May, Basel, Switzerland.
Petersen, K. E. (1982). *Proc. IEEE*, **70**, 420–457.
Shah, J. S. & Straumanis, M. E. (1972). *Solid State Commun.* **10**, 159–162.
Stimson, J., Docker, P., Ward, M., Kay, J., Chapon, L. & Diaz-Moreno, S. (2017). *IOP Conf. Ser. Mater. Sci. Eng.* **278**, 012055.
Tipler, P. A. (1999). *Physics for Scientists and Engineers*. New York: W. H. Freeman/Worth Publishers.
Wilson, E. J. N. (1996). *Proceedings of the 5th European Particle Accelerator Conference (EPAC'96)*, 10–14 June 1996, Barcelona, Spain, pp. 135–139. FRX04A.